Molecular Switch Triggered by Solvent Polarity: Synthesis, Acid–Base Behavior, Alkali Metal Ion Complexation, and Crystal Structure

Gianluca Ambrosi,[a] Paolo Dapporto,[b] Mauro Formica,[a] Vieri Fusi,*[a] Luca Giorgi,[a] Annalisa Guerri,[b] Mauro Micheloni,*[a] Paola Paoli,[b] Roberto Pontellini,[a] and Patrizia Rossi[b]

Abstract: The synthesis and characterization of the new tetraazamacrocycle L, bearing two 1,1′-bis(2-phenol) groups as side-arms, is reported. The basicity behavior and the binding properties of L toward alkali metal ions were determined by means of potentiometric measurements in ethanol/water 50:50 (v/v) solution (298.1 ± 0.1 K, I = 0.15 mol dm^{-3}). The anionic $H_{-1}L^-$ species can be obtained in strong alkaline solution, indicating that not all of the acidic protons of L can be removed under the experimental conditions used. This species behaves as a tetraprotic base (log K_1 = 11.22, log K_2 = 9.45, log K_3 = 7.07, log K_4 = 5.08), and binds alkali metal ions to form neutral $[MH_{-1}L]$ complexes with the following stability constants: log K_{Li} = 3.92, log K_{Na} = 3.54, log K_K = 3.29, log K_{Cs} = 3.53. The arrangement of the acidic protons in the $H_{-1}L^-$ species depends on the polarity of the solvents used, and at least one proton switches from the amine moiety to the aromatic part upon decreasing the polarity of the solvent. In this way two different binding areas, modulated by the polarity of solvents, are possible in L. One area is preferred by alkali metal ions in polar solvents, the second one is preferred in solvents with low polarity. Thus, the metal ion can switch from one location to the other in the ligand, modulated by the polarity of the environment. A strong hydrogen-bonding network should preorganize the ligand for coordination, as confirmed by MD simulations. The crystal structure of the $[Na(H_{-1}L)]\cdot CH_3CN$ complex (space group $P2_1/c$, a = 12.805(1), b = 20.205(3), c = 14.170(2) Å, β = 100.77(1)°, V = 3601.6(8) Å^3, Z = 4, R = 0.0430, $wR2$ = 0.1181), obtained using CH_2Cl_2/CH_3CN as mixed solvent, supports this last aspect and shows one of the proposed binding areas.

Keywords: alkali metals · molecular dynamics · molecular switches · structure elucidation · synthesis

Introduction

Macrocyclic compounds continue to attract the interest of researchers in coordination chemistry.[1–5] Indeed, the countless possible applications of these molecules, as well as their usefulness in fundamental studies, have made this a thriving field of research.[6–10] The synthesis of molecular switches is a growing area because of the potential of these related systems for use in carrying information and, eventually, in molecular devices.[11] Several examples are based on systems whose optical properties (such as photochromism, luminescence, optical nonlinearity) can be switched or modulated by external stimulation such as chemical,[12] electrochemical,[13] and light inputs.[14] However, researchers in many other fields are interested in applying these systems for molecular recognition or in coordination chemistry, in which the system switches adapting (or not) itself to recognize the substrate.[15]

Over the last few years, we have synthesized many cyclic (macrocycles) and noncyclic ligands with one phenolic function in their molecular framework.[16] Clearly many different molecular topologies are possible; however, the insertion of the phenolic group always strongly influences the coordination and spectroscopic properties of the resulting molecule. By joining phenolic oxygen with amine-nitrogen donor atoms, it is possible to produce an internal separation of negative and positive charges in the ligands depending on pH values in aqueous solution;[17] in many cases, one of the acidic protons in the free ligand or in the complex formed can switch its position from a nitrogen to the oxygen atom of the phenol and vice-versa, depending on the polarity of the solvent used.[18] Moreover, when these ligands have lost all acidic protons, they have a harder oxygen atom in the phenolate group with softer amine nitrogen atoms. These aspects led us

[a] Prof. V. Fusi, Prof. M. Micheloni, Dr. G. Ambrosi, Dr. M. Formica, Dr. L. Giorgi, Dr. R. Pontellini
Istituto di Scienze Chimiche, Università di Urbino
Piazza Rinascimento 6, 61029 Urbino (Italy)
Fax: (+39) 0722-350032
E-mail: vieri@chim.uniurb.it

[b] Prof. P. Dapporto, Dr. A. Guerri, Prof. P. Paoli, Dr. P. Rossi
Dipartimento di Energetica "S. Stecco", Università di Firenze
via S. Marta 3, 50139 Firenze (Italy)

0947-6539/03/0903-0800 $ 20.00+.50/0

to increase the number of phenolic groups while preserving a high number of amine functions, with the aim of creating softer and harder coordination areas in the ligand, and a high number of spatially separated negative and positive charges. Furthermore, the idea was to modulate these properties by acting on the surrounding environment, by means of the pH and/or the polarity of the medium, causing the ligand to adapt to fulfil a specific purpose. Indeed, changes in the environment can produce profound modifications in the molecule, forcing not only the protons but also a coordinated metal ion to move from one region of the molecule to another, producing a molecular switch. We recently reported a synthetic pathway for the production of aza-macrocycles containing a 1,1′-bis(2-phenol) fragment with two contiguous phenolic groups.[19] Taking into account that no examples of the coordination properties of biphenol toward metal cations and only very few examples of it as an integral part of ligands had previously been reported,[20] its coordination behavior appeared interesting.

Herein we report the synthesis of the new ligand 1,7-bis[(2,2′-dihydroxybiphen-3-yl)methyl]-4,10-dimethyl-1,4,7,10-tetraazacyclododecane (L). Ligand L was synthesized by attaching two 1,1′-bis(2-phenol) groups to a tetraaza macrocycle. In this way we introduced a high number of phenolic groups into an amine skeleton capable of producing two different hard and soft coordination areas. Moreover, a high degree of separation of positive and negative charges was achieved. The basicity and binding properties of L towards alkali metal ions were investigated in solvents with different dielectric constants.

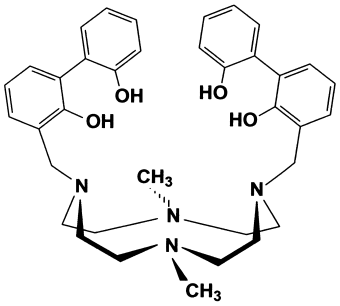

1

Results and Discussion

Synthesis: The synthetic pathway used to obtain L is depicted in Scheme 1. The reagent 3-bromomethyl-2,2′-dimethoxybiphenyl (**3**) was synthesized starting from 1,1′-biphenol, the hydroxy functions of which were protected with methyl groups to give **1** as previously reported. The aromatic ring was activated at the 3 and 3′ positions by using butyllithium and a methyl group was inserted by using dimethyl sulfate in THF to give **2**. The same reaction performed in diethyl ether gave lower yield. The inserted methyl group was brominated by using *N*-bromosuccinimide to afford the reagent **3**. The macrocycle **5** was obtained in high yield by reacting two equivalents of **3** with the tetraaza macrocyclic base **4** in CH_3CN in the presence of a base. The demethylation of the phenolic oxygen atom was carried out with a 48% acetic acid/HBr mixture in the presence of phenol, affording macrocycle L as the tetrahydrobromide salt, which was further purified by recrystallization from methanol–acetonitrile solution. Other cleavage reactions of the methyl groups, using BBr_3, $LiAlH_4$, or lithium in liquid NH_3, led to an uncontrolled reaction.

X-ray structure of [Na(H$_{-1}$L)]·CH$_3$CN (6): The asymmetric unit of $[Na(H_{-1}L)] \cdot CH_3CN$ (**6**) contains a molecule of **6** and a molecule of CH_3CN, which are not involved in relevant intramolecular contacts. The sodium cation is hexacoordinated by the four nitrogen atoms and the O1 and O3 oxygen atoms of L. The coordination polyhedron can be described as a distorted trigonal prism with the O1, N1, N2 and O3, N3, N4 atoms defining the two triangular faces, which are parallel within 6.94(6)° (Figure 1, Table 1). The Na–N distances fall in the range 2.467(2)–2.520(2) Å and are significantly shorter than those found for sodium complexes of cyclen derivatives (a search performed in the Cambridge Structural database (CSD) v5.22[21] showed that the range for Na–N distances in the 13 complexes retrieved is 2.532–2.726 Å). The two Na–O

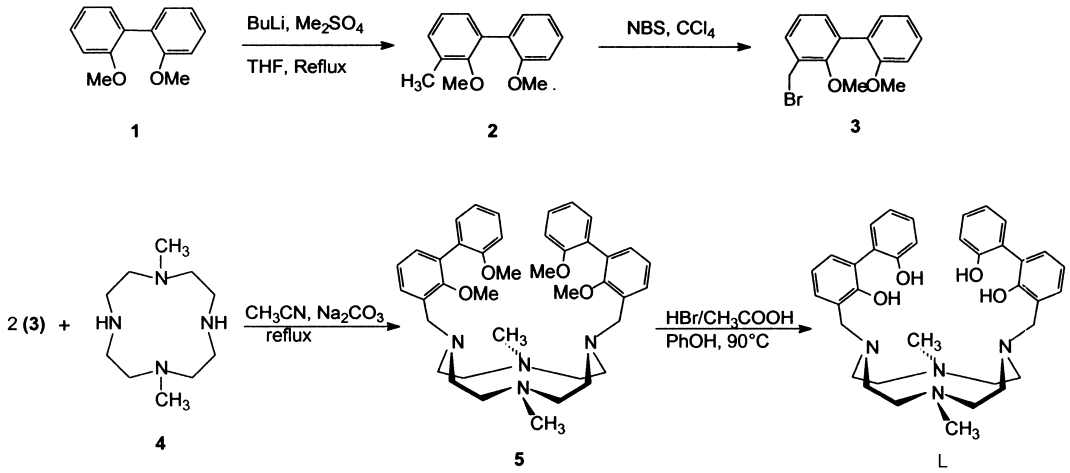

Scheme 1. Synthesis of L.

  0947-6539/03/0903-0801 $ 20.00+.50/0

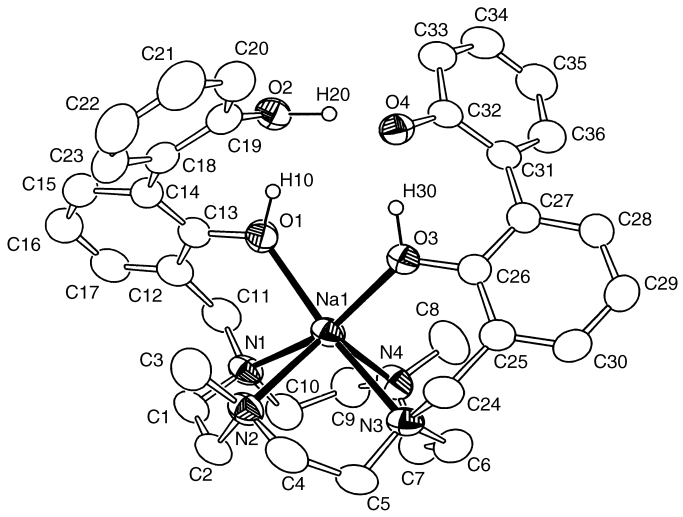

Figure 1. Structure of compound **6** (ORTEP view).

Table 1. Selected bond lengths [Å] and angles [°] for **6**.

Na1–O3	2.303(2)	Na1–O1	2.320(2)
Na1–N2	2.467(2)	Na1–N4	2.470(2)
Na1–N3	2.519(2)	Na1–N1	2.520(2)
O3-Na1-O1	85.82(5)	O3-Na1-N2	120.08(6)
O1-Na1-N2	101.49(6)	O3-Na1-N4	106.13(6)
O1-Na1-N4	124.35(6)	N2-Na1-N4	116.35(6)
O3-Na1-N3	80.13(5)	O1-Na1-N3	160.68(6)
N2-Na1-N3	74.75(6)	N4-Na1-N3	72.78(6)
O3-Na1-N1	160.75(6)	O1-Na1-N1	7.92(6)
N2-Na1-N1	73.84(6)	N4-Na1-N1	75.58(6)
N3-Na1-N1	117.98(6)		

distances (2.320 and 2.303 Å) are also slightly shorter than those observed for sodium complexes with 2,2′-binaphthol derivatives (seven sodium complexes with Na–O distances in the 2.363 – 2.568 Å range were found in the CSD). Concerning the conformation adopted by the biphenol moieties, we found that the angles between the aromatic ring of the binaphthyl units are 45.04(6) and 38.83(6)° for (C12 – C17)-(C18 – C23) and (C25 – C30-(C31 – C36), respectively.

To investigate the coordination behavior of L, the solid-state structures of alkali cation complexes with the macrocyclic ligand framework outlined in Scheme 2a were looked up in the CSD. The structure of a binuclear lithium – boron complex[22] with the 1,7-aza,4-11-oxacyclododecane derivative shown in Scheme 2b (from now on deonted as $LiBN_2O_6$) was

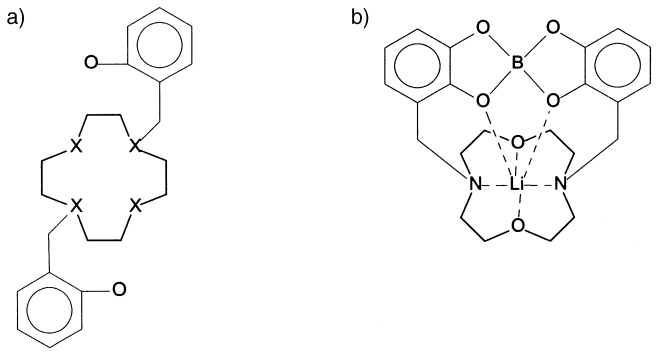

Scheme 2. a) Searched ligand in CSD (X = O, N). b) $LiBN_2O_6$.

retrieved. The overall structures of **6** and $LiBN_2O_6$ are very similar in that both feature: 1) the quite common [3333] C corners[23] conformation for the [12]aneN_4[24] and [12]aneN_2O_2 rings; 2) the aromatic arms folded towards the macrocyclic cavity with a head-to-tail arrangement; 3) a very similar coordination polyhedron around the two alkali cations. This similarity may be ascribed to the intramolecular interaction involving the oxygen atoms of the aromatic moieties. In fact, in compound **6** there are three short intramolecular hydrogen bonds (Table 2) that involve two oxygen atoms (O2 and O4) and three hydrogen atoms (H10, H20, and H30). Interestingly, the O2–H20 and O4–H20 distances are comparable, that is the H20 atom is almost equidistant, within 3σ, between O2 and O4, whereas in $LiBO_6N_2$ the four oxygen atoms of the catechol moieties are held together by the boron atom. In the solid-state structure of compound **6** no relevant intermolecular contacts are present.

Table 2. Intramolecular hydrogen-bond lengths [Å] and angles [°] for compound **6**.

O1–H10	0.95(3)	H10 ··· O2	1.65(3)
O2–H20	1.14(4)	H20 ··· O4	1.36(4)
O3–H30	0.99(3)	H30 ··· O4	1.51(3)
		O1–H10 ··· O2	166(3)
		O2–H20 ··· O4	167(3)
		O3–H30 ··· O4	170(3)

Solution studies, basicity

Potentiometric study: Table 3 summarizes the basicity constants of L, potentiometrically determined in 0.15 mol dm^{-3} NMe_4Cl ethanol/water 50:50 (v/v) solution at 298.1 K. The mixed solvent was used to increase the solubility of the species

Table 3. Basicity constants (Log *K*) of L determined in 50:50 (v/v) H_2O/EtOH (0.15 mol dm^{-3} NMe_4Cl) at 298.1 K.

Reaction	log *K*
$H_{-1}L^- + H^+ \rightarrow L$	11.22(1)
$L + H^+ \rightarrow HL^+$	9.45(1)
$HL^+ + H^+ \rightarrow H_2L^{2+}$	7.07(1)
$H_2L^{2+} + H^+ \rightarrow H_3L^{3+}$	5.08(1)

of L at around pH 7 in aqueous solution. The neutral form of the ligand can, in principle, add four protons and dissociate four protons; it behaves as a triprotic base and as a monoprotic acid under the experimental conditions used. Taking into account that the total number of sites on the ligand that can be involved in the acid – base processes is eight (four nitrogen and four oxygen atoms), the acid – base behavior of L is rather unexpected. In fact, only four of the sites are directly involved under our experimental conditions. As shown in Table 3, L can be present in alkali solution as the species $H_{-1}L^-$. Analyzing the protonation constants starting from this anionic species, it was found that $H_{-1}L^-$ behaves as a rather strong base in the first protonation step (log = 11.22) and the basicity is rather regularly reduced by roughly two log units for each step of protonation, as expected from the increase in the positive charge's repulsion as the molecule

0947-6539/03/0903-0802 $ 20.00+.50/0 *Chem. Eur. J.* **2003**, *9*, No. 3

becomes more protonated. The last three acidic protons present on the $H_{-1}L^{-1}$ species could not be removed under our experimental conditions, suggesting a strong hydrogen-bonding network, which stabilizes them in the molecule.

UV/Vis and NMR spectroscopic studies: UV/Vis absorption electronic spectra of L were obtained in ethanol/water solvent at different pH values to determine the role of the phenolic function in the acid–base behavior of L. The spectra show different wavelength maxima (λ_{max}) in the field of pH 2 and 12.5. At pH 2 the H_3L^{3+} species is prevalent in solution, and two bands with $\lambda_{max} = 242$ and 283 nm, having molar absorptivities of $\varepsilon = 7400$ and 6900 $cm^{-1}mol^{-1}dm^3$ respectively, were observed. At pH 12.5 the $H_{-1}L^{-}$ species is prevalent in solution, and the spectrum mainly exhibits one band at $\lambda_{max} =$ 316 nm ($\varepsilon = 8500\ cm^{-1}mol^{-1}dm^3$). These differences are due to the deprotonation of the phenolic group that occurred at high pH values. In other words, the change in λ_{max} is ascribed to the presence of the phenol hydroxyl form at low pH values and to the phenolate form at high pH values. By monitoring the spectra on going from acidic to basic pH and plotting the absorbance of the spectra at $\lambda = 316$ nm (Figure 2, ■) versus

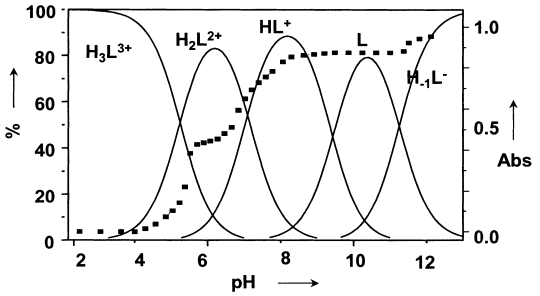

Figure 2. Absorbance values at $\lambda = 316$ nm (■) and distribution diagram of the protonated species (–) of L as a function of pH, in 50:50 (v/v) ethanol/water solution at 298.1 ± 0.1 K with 0.15 mol dm^{-3} Me_4NCl as ionic medium.

pH, it is possible to determine during which deprotonation steps the biphenols lose the acidic protons. This is possible by coupling the trend of the value of the absorbance ascribed to the involvement of the chromophores in the deprotonation processes with the distribution diagram of the species obtained by potentiometric measurements (lines in Figure 2). The absorbance at 316 nm is approximately zero at pH < 4, while it increases at higher pH, reaching its maximum values at pH 12.5. Taken together with the distribution diagram of the species, the absorbance was found to increase with the appearance of the H_2L^{2+} species, reaching a plateau from approximately pH 5.8 to pH 6.5, then increasing again with the appearance of the HL^+ species, and finally reaching another plateau from pH 8.5 to pH 11.3. It was also found to be only slightly perturbed in the presence of the $H_{-1}L^{-}$ species. Taking into account that the change in absorbance is due to the deprotonation of phenol groups, this profile can be attributed to a first deprotonation of the chromophores that occurred in the H_2L^{2+} species ($\varepsilon_{(\lambda=316)} \approx$ 3900 $cm^{-1}mol^{-1}dm^3$) and a second deprotonation in HL^+ ($\varepsilon_{(\lambda=316)} \approx 7800\ cm^{-1}mol^{-1}dm^3$), while a very limited involvement of the chromophores can be supposed in the $H_{-1}L^{-}$ species. In the spectra recorded in the presence of an excess of NMe_4OH, further changes were not observed, suggesting that no other deprotonation process occurs in the chromophores even at higher pH values.

These data can be merged with those obtained in ^1H and ^{13}C NMR experiments performed at different pH values in CD_3OD/D_2O 50/50 (v/v) mixed solvent, which furnished more information about the localization of the acidic protons in the different protonated species; $^1H-^1H$ and $^1H-^{13}C$ NMR correlation experiments were performed to assign all of the signals. The trends in chemical shifts of the most significant resonances, reported as a function of pH, are shown in Figures 3a and 3b. The ^{13}C NMR spectrum, recorded at pH 3, where H_3L^{3+} is prevalent in solution, exhibits fifteen peaks at $\delta = 42.6$ (C1), 48.4 (C3), 52.8 (C4), 54.7 (C2), 117.2 (C13), 122.9 (C9), 123.2 (C15), 124.8 (C5), 126.2 (C7), 129.3 (C11),

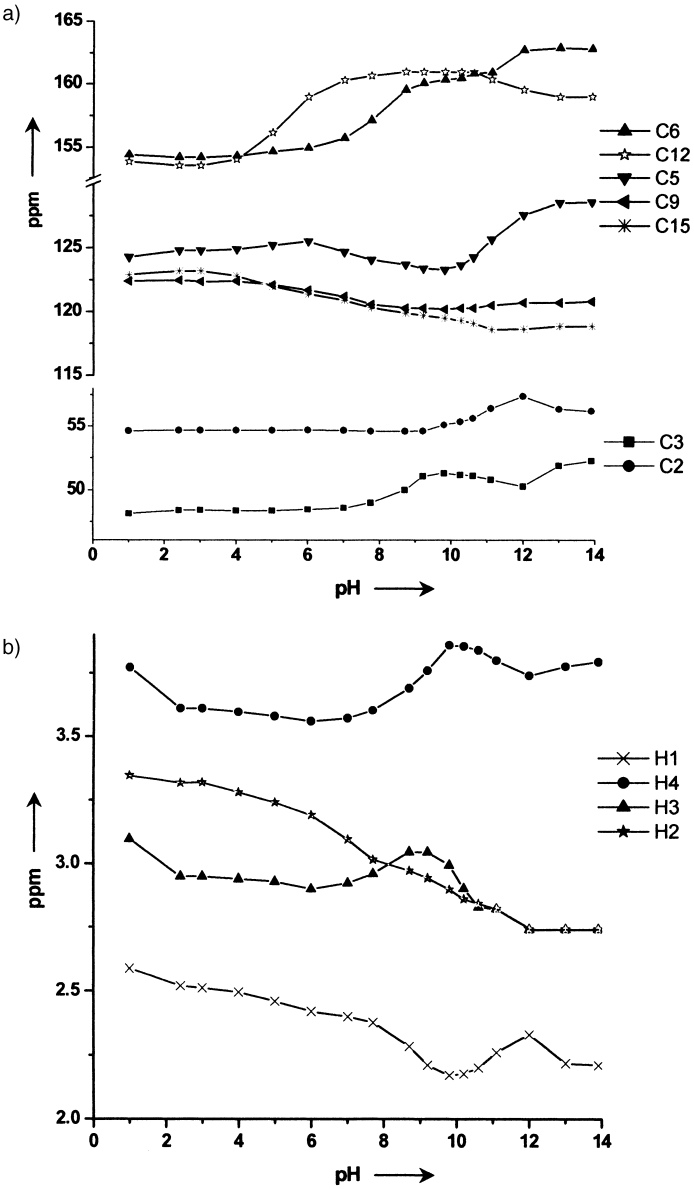

Figure 3. Experimental NMR chemical shifts of L in 50:50 (v/v) CD_3OD/D_2O solution, as a function of pH. a) ^{13}C NMR ; b) ^1H NMR.

  0947-6539/03/0903-0803 $ 20.00+.50/0

131.4 (C14), 133.3 (C16), 133.5 (C8, C10), 153.5 (C12), and 154.2 ppm (C6). The ^{1}H NMR spectrum has a singlet at $\delta =$ 2.52 ppm, which integrates for six protons and is due to the resonance signals of the H1 protons, a multiplet at $\delta =$ 2.95 ppm (8H, H3), a multiplet at $\delta = 3.31$ ppm (8H, H2), a singlet at $\delta = 3.61$ ppm (4H, H4), a multiplet at $\delta = 6.97$ ppm (6H, H9, H13, H15), and a multiplet at $\delta = 7.23$ ppm (8H, H8, H10, H16, H14). The spectrum indicates a C_{2v}-symmetrical structure on the NMR time scale, which is preserved throughout the pH range investigated.

At the lowest pH values, where the fully protonated species H_4L^{4+} should be present in solution, the most significant change is due to the downfield shift of the H3 and H4 protons (see Figure 3b) in the α-position to the nitrogen atoms bearing the side arms, which indicates that the last protonation step needed to obtain the full protonated species H_4L^{4+} takes place on these amine groups. In other words, the H_3L^{3+} species shows a distribution of the seven acidic protons as depicted in Scheme 3. On increasing the pH to the range in which the protonated species H_2L^{2+} is prevalent in solution

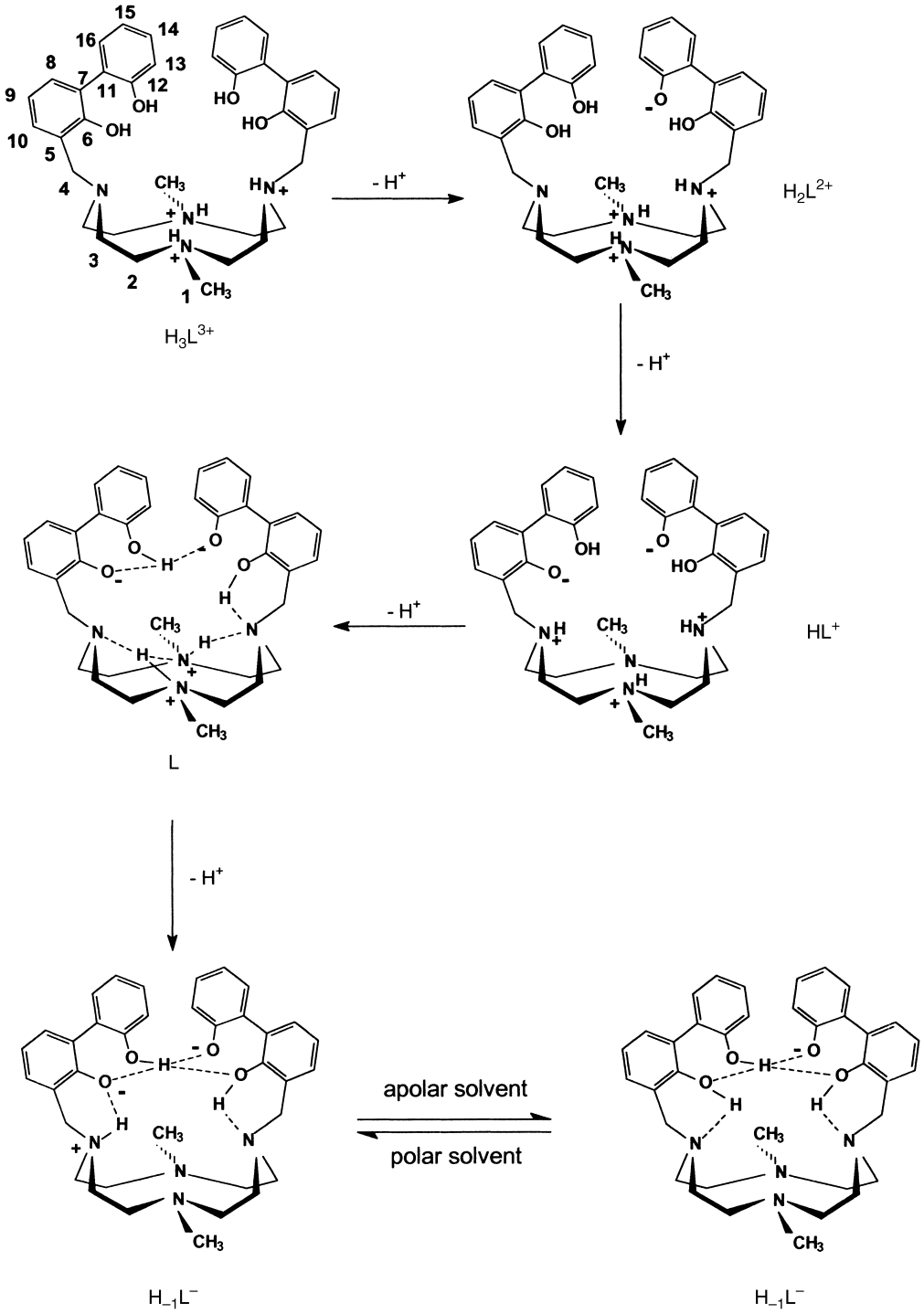

Scheme 3. Location of acidic hydrogen atoms in the protonated species of L.

0947-6539/03/0903-0804 $ 20.00+.50/0 *Chem. Eur. J.* **2003**, *9*, No. 3

(pH 5.5–7), the resonance signal of the aromatic carbon atoms C12 shows a marked downfield shift. In contrast, an upfield shift is observed for the C15 signals in the *para* position to the phenolic oxygen atom (see Figure 3a), suggesting that the deprotonation step takes place on the oxygen atoms of the external phenol groups. This hypothesis is in agreement with the UV/Vis measurements, which indicate the involvement of biphenol chromophores in the deprotonation processes on going from H_3L^{3+} to H_2L^{2+}. In the pH 7.5–9 range, where the HL^+ species is predominant in solution, many resonance signals undergo a shift. In the ^{13}C NMR, the most relevant shifts are due to the C6 and C3 resonance signals, which shift downfield, and C2, C5, and C9, which shift upfield. This contrasting behavior can be explained by taking into account that the UV/Vis measurements suggest a further involvement of the phenol moieties in this deprotonation step as well. Thus the deprotonation must take place on the oxygen atom with C6 in the α-position, and as a result of the effect of the deprotonation on the carbon signals of the phenol, the signal of C6 shifts downfield, while C5 and C9 in the *ortho* and *para* position, respectively, shift upfield.[25] The shifts of C2 and C3 can be explained, in agreement with the β-effect of the protonation of the polyamines,[26] by a redistribution of one positive charge in the macrocyclic base, which shifts from the methylated nitrogen atoms to the nitrogen atoms bearing the biphenols. This leads to the proton distribution depicted in Scheme 3. This hypothesis was confirmed by the trend of the ^1H NMR aliphatic resonance signals which, in the pH 7.5–9 range, show an upfield shift of the signal of the H1 and H2 hydrogen atoms, while the resonance signals of H4 and H3 shift downfield. Examination of the spectra recorded in the pH range where the neutral species L is prevalent ($10 < pH < 11$), revealed that the main resonance signals moving in the ^{13}C NMR spectra are the resonance signals of C5 and C2, which shift downfield, and C3, which shifts upfield. The trend in the shift of C5 and C2 suggests, as does the β-effect of the deprotonation of the polyamines, the involvement of the nitrogen bearing the side arms in the deprotonation process. In contrast, the trend of C3 leads us to suppose a new redistribution of charge involving the protons located on the polyamine base, which increase the positive charge on the methylated nitrogen atoms and produce a downfield shift of the resonance signal of C3. This hypothesis is in agreement with the simultaneous upfield shift of the H4 and H3 resonance signals and the downfield shift of H1 in the ^1H NMR experiments. This behavior fits well with the UV/Vis measurements, in which the involvement of the chromophores was not detected, indicating that the deprotonation must occur on the macrocyclic base.

The last deprotonation step detected by means of potentiometric measurements forms the anionic $H_{-1}L^-$ species and occurs up to pH 11. In the formation of this species, the most relevant changes are due to the signals of C2 and C3, which again show contrasting behavior, shifting upfield and downfield, respectively. The most important changes in the ^1H NMR spectrum are the upfield shift of H1 and the downfield shift of H4. This trend could be explained by the involvement of the amine base in this deprotonation step as well, which leads to a distribution of charge as depicted in Scheme 3. However, the aromatic parts undergo perturbation, as visible by the shift of the signals due to C6 and C12 and by the UV/Vis experiments. Further addition of a base did not produce substantial changes in the NMR spectra, indicating that the three acidic proton residues are strongly stabilized, probably because of a dense hydrogen-bonding network, as suggested in Scheme 3 for the $H_{-1}L^-$ species. Scheme 3 depicts the complete distribution of the acidic protons in the different protonated species proposed by the UV/Vis and NMR experiments.

As can be seen in Scheme 3, L shows an internal separation of positive and negative charges in the species existing up to pH 5. For example, the neutral species L has two ammonium and two phenolate groups.

In conclusion, the insertion of two biphenol groups into a polyamine macrocycle influences the disposition of the acidic protons, permitting a separation of the positive and negative charges in the polyprotonated species even at slightly acidic pH values. For this reason, L offers promising possibilities for use as a receptor for substrates, such as the simple amino acids, which present a simultaneous separation of negative and positive charges.

The anionic species $H_{-1}L^-$ and the neutral species L are also soluble in organic solvents with a lower dielectric constant, such as $CHCl_3$ or CH_2Cl_2. The spectra of the two species in $CHCl_3$ show approximately the same profile, with two bands at 283 ($\varepsilon \approx 5000\ cm^{-1}\,mol^{-1}\,dm^3$) and 316 nm ($\varepsilon \approx 3700\ cm^{-1}\,mol^{-1}\,dm^3$) characteristic of the simultaneous presence of the phenolic and phenolate forms of the chromophores. The molar absorptivities, compared with those previously reported for the polar mixed solvent, indicate the deprotonation of one phenol group; thus, as reported in Scheme 3, it is possible to hypothesize a redistribution of the acidic protons of $H_{-1}L^-$ in solvents with low dielectric constants. This distribution could easily be obtained by the shift of the acidic proton located in the polyamine base in a polar solvent. In this case, the low solvation power of an apolar solvent leads to a lower separation of charge.

The NMR experiments confirmed this hypothesis. In fact, comparison of the ^1H NMR spectrum of the $H_{-1}L^-$ species recorded in a mixed polar solvent, such as as D_2O/CD_3OD, with that of the same species recorded in $CDCl_3$ revealed a downfield shift of some of aromatic resonance signals in apolar solvents coupled with an upfield shift of the aliphatic resonance signals (Figure 4). These ^1H NMR shifts indicate the transfer of a positive charge density, which is due to an acidic proton that moves from the amine base to the aromatic part going from D_2O/CD_3OD to $CDCl_3$ solution. This internal switch of acidic protons from one part of the molecule to another could be used in molecular recognition to adapt the receptor by changing the polarity of the solvent, as well as to transport information by modulating the environment.[27]

Molecular dynamics (MD) simulation: Starting from the results obtained from the UV/Vis and NMR experiments, MD calculations were performed on the anionic $H_{-1}L^-$ species. In particular, in solvents with a low dielectric constant the acidic hydrogen atoms are bonded to three out of four oxygen atoms of the biphenyl moieties. This implies two different arrange-

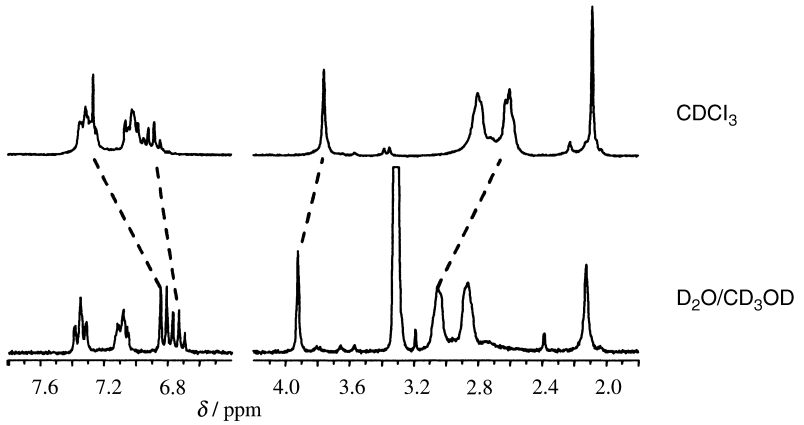

Figure 4. ^{1}H NMR spectra of the $H_{-1}L^-$ species in 50:50 (v/v) CD_3OD/D_2O solution, or in $CDCl_3$.

ments; the negatively charged oxygen atom could be connected to either the phenyl group close to or that far from the cyclen ring (Scheme 4). In the following, these two possible anions were named L123 and L234, where the three numbers stand for the protonated oxygen atoms.

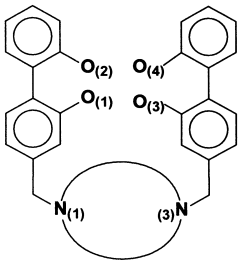

L123	L234	L12*	L13*	L14*	L23*	L24*	L34*
O1-H	O1$^-$	O1-H	O1-H	O1-H	O1$^-$	O1$^-$	O1$^-$
O2-H	O2-H	O2-H	O2-H	O2$^-$	O2-H	O2-H	O2$^-$
O3-H	O3-H	O3$^-$	O3-H	O3$^-$	O3-H	O3$^-$	O3-H
O4$^-$	O4-H	O4$^-$	O4$^-$	O4-H	O4$^-$	O4-H	O4-H

Scheme 4. Location of the acidic hydrogen atoms in the species studied by MD. * denotes that the third hydrogen is bound to N1.

In solvents with high dielectric constants, the three acidic hydrogens are localized on a nitrogen atom bearing the biphenol (Scheme 3) and on two oxygen atoms; as a consequence six different anions result. As above, the resulting anions are named with the letter L and two numbers referring to the two protonated oxygen atoms (L12, L13, L14, L23, L24, and L34, see Scheme 4).

When the dielectric constant was set to 1 and 4.8, only the anions L123 and L234 where investigated. On the other hand, for $\varepsilon = 52.5$ and $\varepsilon = 80$, MD simulations were performed on L12, L13, L14, L23, L24, and L34. For every MD run only the conformations within 10 kcal mol^{-1} of the energy minimum were analyzed. Results are summarized below:

1) Concerning the position of the acidic hydrogen atoms in the anion studied, it has been found that in polar solvents the protonation hydrogen-atom distribution proposed as a result of the UV/Vis and NMR experiments gives rise to the most stable species (L23). In apolar solvent and in vacuum the situation is more complicated and two possible dispositions (L123 and L234) have comparable energies.
2) Many hydrogen bonds are present: as donor and acceptor atoms they involve the oxygen atoms of the biphenolate moieties and the nitrogen atoms bearing the biphenol side arms. As expected, by increasing the dielectric constant of the medium the number of hydrogen bonds decreases. Notably, no hydrogen bonds were detected between the two biphenolate moieties, meaning that the two aromatic side arms appear not to interact with each other. We can thus suppose that the dense hydrogen-bonding network stabilizing the three acidic hydrogen atoms of the $H_{-1}L^-$ species should be confined to each nitrogen atom and to the corresponding linked aromatic side arm. Given this, the short interaction between the oxygen atom O4 and the hydrogen atom bonded to O2 (see Table 2, and Figure 1) found in the solid-state structure of the complex $[Na(H_{-1}L)]\cdot CH_3CN$ could be a consequence of the coordinated sodium cation, which forces the two biphenolate moieties close to each other, acting as a bridge between the two aromatic arms.
3) No $\pi-\pi$ stacking interactions were found, confirming the idea that the biphenolate moieties act separately.

Alkali metal ion complexation: The coordination characteristics of L towards the alkali metal ions Li^+, Na^+, K^+, and Cs^+ were studied in 0.15 mol dm^{-3} NMe_4Cl, ethanol/water 50:50 (v/v) solution as mixed solvent at 298.1 K. The stability constants for the equilibrium reactions of L were determined potentiometrically and are reported in Table 4. L forms only mononuclear species with $[MH_{-1}L]$ stoichiometry with all four of the ions examined. The addition constants of the metal to the $H_{-1}L^-$ species are almost the same for the four metals, resulting in a log K value of about 3.5 logarithmic units for each addition constant. Taking into account that the macrocyclic base does not bind alkali metal ions under these experimental conditions, the binding capabilities of L together with the absence of selectivity towards these alkali ions must be attributed to the high adaptability of the side arms to coordination, which permits binding of the metals but does not discriminate among them. In other words, considering that

Table 4. Logarithms of the equilibrium constants determined in 50:50 (v/v) H_2O/EtOH (0.15 mol dm^{-3} NMe_4Cl) at 298.1 K for the complexation reactions of L with Li^+, Na^+, K^+, and Cs^+ ions.

	Li^+	Na^+	K^+	Cs^+
Reaction $H_{-1}L^- + M^+ \rightarrow [MH_{-1}L]$	3.92	3.54	3.29	3.53

0947-6539/03/0903-0806 $ 20.00+.50/0 *Chem. Eur. J.* **2003**, *9*, No. 3

coordination in these cases is essentially due to electrostatic forces, it is possible to suppose that the side arms are preorganized by the macrocyclic skeleton to coordinate the metal ions and that they easily adapt around the metals. It is noteworthy that coordination occurs only with the monoanionic species, forming neutral complexes. These species are also soluble in organic solvents with lower dielectric constants than the mixed solvent used for the potentiometric measurements.

Interestingly, L can stabilize the metal ions essentially in two binding areas. One is formed by the tetraamine base and by two oxygen atoms of the two linked biphenol groups that are closer to the macrocyclic base; the other one is formed by the four oxygen atoms of the biphenol chromophores. To identify the active binding area for the alkali metal ions in solution and to determine if a change of solvent produces a change in the active binding area, UV/Vis and NMR spectra of the $[MH_{-1}L]$ species were obtained and compared with those of the $H_{-1}L^-$ species recorded under the same experimental conditions. The mixed solvent used for the potentiometric measurements and solvents having lower dielectric constant were investigated.

No marked differences in absorbance or in λ_{max} were found between the spectrum of L recorded at pH 13 in H_2O/EtOH, where the $H_{-1}L^-$ is prevalent in solution, with that recorded at pH 13 in the presence of ten equivalents of Na^+ ion to completely form the $[NaH_{-1}L]$ complex. This indicates that the complexation of sodium does not perturb the optical properties of the chromophores. Because at least one amine function in the $H_{-1}L^-$ species bears a positive charge, the sodium cation cannot be stabilized in that area. The binding area in this mixed polar solvent must thus be formed by the four phenol oxygen atoms, in which there is a high density of negative charges, resulting in an arrangement similar to that depicted in Figure 5a. This hypothesis was confirmed by the ^1H NMR spectrum of the sodium complex, in which the peaks of the complex in the aromatic region are perturbed in comparison with those in the spectrum of the $H_{-1}L^-$ species, while there are no substantial differences between the aliphatic regions in the two spectra. Comparison of the spectra of the $H_{-1}L^-$ and $[NaH_{-1}L]$ species in solvents with lower polarity, for example CH_2Cl_2 or $CHCl_3$, showed that the complexation of sodium ion does not influence the chromophores of L, and that the spectra essentially preserve the same profile for the two species. Given the distribution of the acidic protons in these solvents, as discussed above, it is possible that in these solvents the sodium ion is lodged and stabilized by the four amine functions of the macrocyclic base and by the two oxygen atoms of the two closer phenol groups in an arrangement similar to that found in the crystal structure of the sodium complex obtained from CH_2Cl_2 as solvent.

This hypothesis was also confirmed by ^1H and ^{13}C NMR experiments. For example, Figure 6, which shows the two spectra of the $[NaH_{-1}L]$ species recorded in $CDCl_3$ or in the mixed solvent D_2O/CD_3OD 50:50 (v/v), highlights

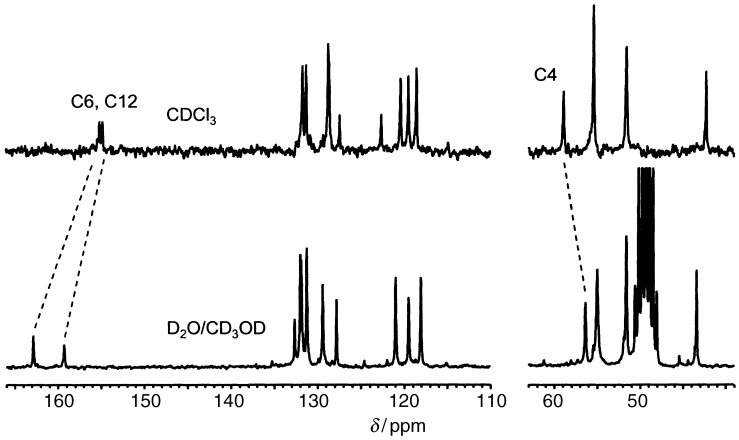

Figure 6. ^{13}C NMR spectra of the $[NaH_{-1}L]$ complex in 50:50 (v/v) CD_3OD/D_2O, or in $CDCl_3$ solution.

the different distribution of positive charges present in the two solvents. In particular, in $CDCl_3$ the biphenol groups show the presence of more intact phenol groups than in the mixed solvent D_2O/CD_3OD (C6, C12 shift upfield in $CDCl_3$), while the amine base is richer in positive charge in D_2O/CD_3OD (C4 shift upfield in D_2O/CD_3OD). The UV/Vis and NMR experiments performed in water or in pure alcohol solvent revealed the same behaviors and also gave similar results with the complexes of Li^+, K^+, and Cs^+.

In conclusion, in solvents with high dielectric constants, such as water, alcohol, or their mixtures, the binding area is formed by the oxygen atoms of the biphenol moieties, which are probably preorganized for coordination by a hydrogen-bonding network involving the amine base. In contrast, in solvents with lower dielectric constants, such as CH_2Cl_2 and $CHCl_3$, the metal switches to another binding area formed by the four amine functions of the macrocyclic base and by two oxygen atoms of the two closer phenol functions. Also in this case, a hydrogen-bonding network can be supposed to preorganize the side arms. L thus shows the attractive property of allowing switching of a metal ion inside it, moving the metal from one part of the molecule to the other by simply changing the dielectric constants of the solvent (Figure 5a and 5b). Again, as in the case of the above proton switch, this mode of complexation opens a route for carrying information using very simple molecules.

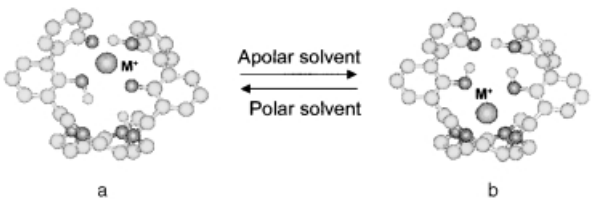

Figure 5. Proposed coordination models of alkali ions in $[MH_{-1}L]$ species in a) polar solvents, b) apolar solvents.

  0947-6539/03/0903-0807 $ 20.00+.50/0

Conclusion

The molecular topology of ligand L is characterized by the a tetraamine macrocyclic skeleton on which two 1,1′-bis(2-phenol) moieties were attached as side-arms. L does not lose three of its acidic protons in ethanol/water 50:50 (v/v) solution, probably because of the strong intramolecular hydrogen-bonding network in which they are involved. The disposition of the acidic protons in the several species produces separation of negative and positive charges in the ligand in ethanol/water solution. Moreover the acidic protons in the neutral and anionic $H_{-1}L^{-}$ species show different disposition in solvents with high dielectric constants, such as water or ethanol, than in solvents having lower polarity, such as $CHCl_3$. At least one proton switches from the macrocyclic base towards the aromatic side arms on decreasing the polarity of the solvent. For this reason, this internal proton switch cannnot only be used as receptor for substrates with an internal separation of charge, but can also be adapted to the substrate in molecular recognition by modulation of the polarity of the medium.

L binds one alkali metal ion in alcohol/water 50:50 (v/v) solution and in organic solvents. The ligand does not show selectivity towards the metal ions, but the neutral complexes obtained are soluble in organic solvents; thus L could be used to extract such metal ions from their aqueous solution. The experiments performed suggest that the metal can move within the complex, switching from a coordination area formed by the four oxygen atoms of the biphenol moieties in polar solvents to an area formed by the tetraamine functions and by two oxygen atoms of the two closer phenol functions in apolar solvents. This effect, as in the case of the above proton switch, opens the way to carrying information using a very simple molecule.

Experimental Section

General: Ligand L was obtained following the synthetic procedure reported in Scheme 1. 2,2′-Dimethoxydiphenyl (**1**) and 1,4,7,10-tetrazacyclododecane (**4**) were prepared as previously described.[28, 29]. ^{1}H and ^{13}C NMR spectra were recorded on a Bruker AC-200 instrument, operating at 200.13 and 50.33 MHz, respectively. For the ^{1}H NMR experiment, the peak positions are reported with respect to HOD ($\delta = 4.75$ ppm); dioxane was used as the reference standard in ^{13}C NMR spectra ($\delta = 67.4$ ppm) that were obtained in aqueous solution. For the spectra recorded in $CDCl_3$ and CD_3OD, the peak positions are reported with respect to TMS. ^{1}H – ^{1}H and ^{1}H – ^{13}C correlation experiments were performed to assign the signals. IR spectra were recorded on a Shimadzu FTIR-8300 spectrometer. UV/Vis absorption spectra were recorded at 298 K on a Varian Cary-100 spectrophotometer equipped with a temperature control unit. ESI mass spectra were recorded on a ThermoQuest LCQ Duo LC/MS/MS spectrometer. Melting points were determined on a Büchi B-540 apparatus. Solvents and starting materials were used as purchased.

3-Methyl-2,2′-dimethoxybiphenyl (2): A solution of butyllithium (21 mL, 10 M in THF) was added to 2,2′-dimethoxybiphenyl (**1**) (15.0 g, 0,07 mol) dissolved in freshly distilled THF (500 mL). The addition of butyllithium caused vigorous refluxing. The resulting solution was stirred for 30 min and a solution of dimethyl sulfate (26.5 g, 0.21 mol) dissolved in freshly distilled THF (50 mL) was then added dropwise. The addition of dimethyl sulfate caused vigorous refluxing. Excess dimethyl sulfate was destroyed by stirring the organic layer with 1 M NaOH (400 mL). The organic solution was separated, dried over anhydrous Na_2SO_4, and evaporated to dryness to afford a brownish oil. The crude product was chromatographed on silica gel with hexane/ethyl acetate 95:5 as eluent, affording **2** as a white solid (7.83 g, 49 %). M.p. 98 – 100 °C; ^{1}H NMR ($CDCl_3$): $\delta = 2.36$ (s, 3H), 3.42 (s, 3H), 3.81 (s, 3H), 7.2 ppm (m, 7H); MS (ESI): m/z: 229 $[M+H]^+$; elemental analysis calcd (%) for $C_{15}H_{16}O_2$: C 78.92, H 7.06, N 0.00; found: C 79.0, H 7.1, N 0.0.

3-Bromomethyl-2,2′-dimethoxybiphenyl (3): 3-Methyl-2,2′-dimethoxybiphenyl (**2**) (4.6 g, 0.02 mol), *N*-bromosuccinimide (3.9 g, 0.022 mol), and azobisisobutyronitrile (AIBN) (80 mg, 0.5 mmol) were dissolved in CCl_4 (40 mL). The resulting mixture was refluxed for 24 h. The mixture was cooled to room temperature and the solid *N*-succinimmide was filtered off. The organic solution was dried over anhydrous Na_2SO_4 and evaporated to dryness to afford a yellowish oil. The crude product was recrystallized from hot methanol, to afford **3** as a white solid (4.9 g, 80 %). M.p. 156 – 158 °C; ^{1}H NMR ($CDCl_3$): $\delta = 3.48$ (s, 3H), 3.81 (s, 3H), 4.65 (s, 2H), 7.2 ppm (m, 7H); MS (ESI): m/z: 307 – 309 $[M+H]^+$; elemental analysis calcd for $C_{15}H_{15}BrO_2$: C 58.65, H 4.92, N 0.00; found: C 58.8, H 5.0, N 0.0.

1,7-Bis[(2,2′-dimethoxybiphen-3-yl)methyl]-4,10-dimethyl-1,4,7,10-tetraazacyclododecane (5): Amine **4** (1 g, 5 mmol) and Na_2CO_3 (0.5 g, 47 mmol) were suspended in refluxing CH_3CN (100 mL). To this mixture, a solution of **3** (3.07 g, 10 mmol) in CH_3CN (50 mL) was added dropwise over 1 h, after which the suspension was refluxed for 20 h and then filtered. The solution was evaporated under vacuum to yield the crude product, which was chromatographed on neutral alumina ($CHCl_3/CH_3OH$ 10:0.2). The eluted fractions were collected and evaporated to yield **5** as a white solid (2.58 g, 79 %). M.p. 55 – 58 °C; ^{1}H NMR (D_2O, pH 3): $\delta = 2.49$ (s, 6H), 2.79 (brs, 8H), 3.01 (brs, 8H), 3.34 (s, 6H), 3.73 (s, 4H), 3.76 (s, 6H), 7.36 (m, 8H), 6.97 ppm (m, 6H); ^{13}C NMR: $\delta = 43.3$, 50.0, 52.9, 55.4, 56.7, 62.6, 113.0, 122.0, 126.2, 127.5, 131.2, 132.0, 133.7, 134.9, 157.3, 157.6 ppm; MS (ESI): m/z: 654 $[M+H^+]$; elemental analysis calcd for $C_{40}H_{52}N_4O_4$: C 73.59, H 8.03, N 8.58; found: C 73.4, H 8.1, N 8.5.

1,7-Bis[(2,2′-dihydroxy-biphen-3-yl)methyl]-4,10-dimethyl-1,4,7,10-tetraazacyclododecane tetrahydrobromide (L·4HBr): Macrocycle **5** (2.0 g, 3 mmol) and phenol (9.0 g, 96 mmol) were dissolved in HBr/CH_3COOH (33 %, 80 mL). The solution was stirred at 90 °C for 22 h. The resulting suspension was filtered and washed with CH_2Cl_2 several times. The white solid obtained was recrystallized from the CH_3CN/CH_3OH mixture to give L as its tetrahydrobromide salt (1.3 g, 46 %). ^{1}H NMR (D_2O, pH 3, 25 °C): $\delta = 2.64$ (s, 6H), 3.05 (brs, 8H), 3.42 (brs, 8H), 3.72 (s, 4H), 7.14 (m, 8H), 7.36 ppm (t, 6H); ^{13}C NMR $\delta = 42.4$, 48.0, 52.2, 54.3, 117.1, 122.7, 124.5, 125.6, 128.4, 131.4, 133.1, 133.3, 153.0, 153.9 ppm; analysis calcd for $C_{36}H_{48}Br_4N_4O_4$: C 46.98, H 5.26, N 6.09; found: C 47.1, H 5.4, N 6.2.

The neutral species L can easily be obtained in high yield by treating a methanol solution of L·4HBr with a solution of NMe_4OH (1.0 mol dm^{-3}) up to pH 11. Water was added to this solution to complete precipitation of L as a white solid. M.p. 186 °C (decomp); ^{1}H NMR ($CDCl_3$, 25 °C): $\delta = 2.09$ (s, 6H), 2.61 (brs, 8H), 2.80 (brs, 8H), 3.76 (s, 4H), 6.90 (dd, 2H), 7.02 (m, 6H), 7.34 ppm (m, 6H); ^{13}C NMR $\delta = 42.2$, 51.6, 55.4, 58.91, 118.5, 119.4, 120.3, 122.6, 127.4, 128.6, 128.7, 131.2, 131.7, 154.8, 155.2 ppm; MS (ESI): m/z: 598 $[M+H^+]$; elemental analysis calcd for $C_{36}H_{44}N_4O_4$: C 72.46, H 7.43, N 9.39; found: C 72.6, H 7.3, N 9.5.

$[Na(H_{-1}L)]\cdot CH_3CN$ (6): An excess of NaCl was added to a solution of L·4HBr (179 mg, 0.3 mmol) in water (100 mL); NaOH (1 mol dm^{-3}) was added until precipitation of a white solid was complete. The solid was then suspended in $CHCl_3$ (40 mL) and the mixture filtered. The liquid portion was dried over Na_2SO_4 and evaporated to dryness. The solid was recrystallized by slow evaporation of a mixture of CH_2Cl_2/CH_3CN, to give white crystals suitable for X-ray analysis, yield 135 mg (68 %). ^{1}H NMR (CD_3OD, 25 °C): $\delta = 1.98$ (s, 6H), 2.27 (brs, 4H), 2.51 (brs, 12H), 3.62 (s, 4H), 6.69 (t, 4H), 6.81 (d, 2H), 6.93 (d, 2H), 7.09 (t, 2H), 7.30 ppm (d, 4H); ^{13}C NMR: $\delta = 43.3$, 51.6, 55.0, 56.4, 118.0, 119.4, 120.9, 127.8, 129.4, 131.2, 131.8, 131.9, 132.6, 159.3, 162.9 ppm; elemental analysis calcd for $C_{38}H_{46}N_5NaO_4$: C 69.17, H 7.03, N 10.61; found: C 69.2, H 7.1, N 10.5.

Caution: Perchlorate salts of organic compounds are potentially explosive; these compounds must be prepared and handled with great care!

X-ray crystallographic studies on $[Na(H_{-1}L)]\cdot CH_3CN$ (6): For crystal structure determination, cell parameters and intensity data for compound **6** were obtained on a Siemens P4 diffractometer, using graphite-monochromated $Cu_{K\alpha}$ radiation ($\lambda = 1.54184$ Å). Cell parameters were determined by least-squares fitting of 25 centered reflections. The intensities of three

0947-6539/03/0903-0808 $ 20.00+.50/0 *Chem. Eur. J.* **2003**, *9*, No. 3

standard reflections were periodically measured to check the stability of the diffractometer and the decay of the crystal. Intensity data were corrected for Lorentz and polarization effects and an absorption correction was applied once the structure was solved by the method of Walker and Stuart.[30] The structure was solved by using the SIR-97[31] program and subsequently refined by the full-matrix least-squares program SHELX-97.[32] The hydrogen atoms bonded to the oxygen atoms O1, O2, and O3 were found in difference syntheses and their positions and isotropic displacement parameters were refined. All of the other hydrogen atoms were introduced in calculated positions and their coordinates refined in agreement with that of the linked atoms. All of the non-hydrogen atoms were refined anisotropically. Atomic scattering factors and anomalous dispersion corrections for all the atoms were taken from reference [33]. Geometric calculations were performed by PARST97.[34] The molecular plot was produced with the ORTEP-3 program.[35] Crystal and structure refinement data are reported in Table 5.

Table 5. Crystal and structure refinement data for compound **6**.

empirical formula	$C_{38}H_{46}N_5NaO_4$
formula weight	659.79
temperature [K]	298
λ [Å]	1.5418
crystal system	monoclinic
space group	$P2_1/c$
a [Å]	12.805(1)
b [Å]	20.205(3)
c [Å]	14.170(2)
β [°]	100.77(1)
V [Å^3]	3601.6(8)
Z	4
ρ_{calcd} [g cm^{-3}]	1.217
μ [mm^{-1}]	0.740
F(000)	1408
2θ range for data collection [°]	7–120
reflections collected/unique	6944/5758 [R(int) = 0.0159]
data/parameters	4905/450
final R indices [$I > 2\sigma(I)$]	$R1 = 0.0430$, $wR2 = 0.1181$
R indices (all data)	$R1 = 0.0508$, $wR2 = 0.1260$

CCDC-185898 contains the supplementary crystallographic data for this paper. These data can be obtained free of charge via www.ccdc.cam.ac.uk/conts/retrieving.html (or from the Cambridge Crystallographic Data Centre, 12, Union Road, Cambridge CB21EZ, UK; fax: (+44) 1223-336-033; or deposit@ccdc.cam.ac.uk).

Molecular dynamics (MD) simulation protocol: The species studied was the $[H_{-1}L]^-$ ion. The MSI software programs InsightII and Discover version 98.0 were used for all of the molecular modeling studies.[36] The force field used was the ESFF because it has the correct atom type for all of the atoms in the ligand. MD calculations were performed at 300 K and the Verlet leapfrog algorithm, with a time step of 1 fs, was used for integration of equations of motion in all simulations. A distance-dependent dielectric constant was used and set to 1, 4.8, 52.5, and 80 to simulate vacuum, chloroform, water/ethanol (50/50), and water environments, respectively. Before starting each MD procedure the initial anionic species was optimized until the convergence criterion was met (< 0.01 kcal mol^{-1}). For every MD run the system was allowed to equilibrate for 100 ps and then a 1000 ps dynamic study was performed (snapshot conformations were collected every ps). A conformational search was performed to verify the possibility for the aromatic rings belonging to different arms to reach distances compatible with the presence of $\pi-\pi$ stacking interactions. A set of four independent dihedral angles was varied: C13-C12-C11-N1, C13-C14-C18-C19, C26-C25-C24-N3, C26-C27-C31-C32. They were varied in constant steps of 30° in the 0–360° range. This search revealed that only the (C18–C23) and (C31–C36) aromatic rings could have this kind of interaction, because the shortest distance between the (C12–C17) and (C25–C30) rings is 5.8 Å, far longer of an acceptable distance for $\pi-\pi$ stacking interactions (3.3–3.8 Å).[37]

EMF measurements: Equilibrium constants for protonation and complexation reactions with L were determined by pH-metric measurements ($pH = -\log [H^+]$) in 50:50 (v/v) ethanol/water solution at 298.1 ± 0.1 K with 0.15 mol dm^{-3} Me_4NCl as ionic medium, using the fully automatic equipment that has already been described;[38] the EMF data were acquired with the PASAT computer program.[39] The combined glass electrode was calibrated as a hydrogen concentration probe by titrating known amounts of CO_2-free HCl with Me_4NOH solutions and determining the equivalent point by Gran's method,[40] which gives the standard potential E° and the ionic product of water ($pK_w = 14.53(1)$ at 298.1 K in 0.15 mol dm^{-3} Me_4NCl, $K_w = [H^+][OH^-]$) for the mixed solvent EtOH/H_2O. Ligand and metal ion concentrations of $1 \times 10^{-3} - 3 \times 10^{-3}$ were employed in the potentiometric measurements; we performed at least three measurements in the pH 2–11 range. The HYPERQUAD computer program was used to process the potentiometric data.[41] All titrations were treated either as single sets or as separate entities for each system, without significant variation in the values of the constants determined.

Acknowledgement

Financial support from the Italian Ministero dell'Università e della Ricerca Scientifica e Tecnologica (COFIN2000) and CRIST (Centro di cristallografia strutturale) University of Florence are gratefully acknowledged.

[1] a) C. J. Pedersen, *J. Am. Chem. Soc.* **1967**, *89*, 7017; b) D. J. Cram, J. M. Cram, *Science* **1984**, *183*, 4127; c) J.-M. Lehn, *Angew. Chem.* **1988**, *100*, 91; *Angew. Chem. Int. Ed. Engl.* **1988**, *27*, 89; d) P. Guerriero, S. Tamburini, P. A. Vigato, *Coord. Chem. Rev.* **1995**, *110*, 17; e) R. M. Izatt, K. Pawlak, J. S. Bradshaw, *Chem. Rev.* **1995**, *95*, 2529.

[2] a) L.-F. Lindoy, *The Chemistry of Macrocyclic Ligand Complexes*, Cambridge University Press, Cambridge, **1989**; b) J.-S. Bradshaw, *Aza-crown Macrocycles*, Wiley, New York, **1993**; c) P. Dietrich, P. Viout, J.-M. Lehn, *Macrocyclic Chemistry*, VCH, Weinheim, **1993**.

[3] a) N. V. Gerbeleu, V. B. Arion, J. Burgess, *Template Synthesis of Macrocyclic Compounds*, Wiley-VCH, Weinheim, **1999**; b) D. Parker, *Macrocycle Synthesis: a Practical Approach*, Oxford University Press, **1996**.

[4] G. W. Gokel, *Crown Ethers and Cryptands (Monographs in Supramolecular Chemistry)* (Ed.: J. F. Stoddart), The Royal Society of Chemistry, Cambridge, **1992**.

[5] S. Patai, A. Rapport, E. Weber, *Crown Ethers and Analogs*, Wiley, New York, **1998**.

[6] H. J. Schneider, A. Yatsimirsky, *Principles and Methods in Supramolecular Chemistry*, Wiley, Chichester, **2000**.

[7] A. Bianchi, K. Bowman-James, E. Garcia-España, *Supramolecular Chemistry of Anions*, Wiley-VCH, Weinheim, **1997**.

[8] a) A. W. Czarnik, *Fluorescent Chemosensors for Ion and Molecule Recognition*, Am. Chem. Soc., Washington DC, **1993**; b) R. Bergonzi, L. Fabbrizzi, M. Licchelli, C. Mangano, *Coord. Chem. Rev.* **1998**, *170*, 31.

[9] C. Bazzicalupi, A. Bencini, A. Bianchi, V. Fusi, C. Giorgi, A. Masotti, F. Pina, A. Roque, B. Valtancoli, *J. Chem. Soc. Chem. Commun.* **2000**, 561–562.

[10] Y. A. Zoltov, *Macrocyclic Compounds in Analytical Chemistry*, Wiley-Interscience, New York, **1997**.

[11] a) R. Ballardini, V. Balzani, A. Credi, M. T. Gandolfi, M. Venturi, *Struc. Bond.* **2001**, *99*, 163; b) P. Ashton, R. Ballardini, V. Balzani, A. Credi, K. R. Dress, E. Ishow, C. J. Kleverlaan, O. Kocian, J. A. Preece, N. Spencer, J. F. Stoddart, M. Venturi, S. Wenger, *Chem. Eur. J.* **2000**, *6*, 3558; c) V. Amendola, L. Fabbrizzi, C. Mangano, P. Pallavicini, *Acc. Chem. Res.* **2001**, *34*, 488; d) R. Ballardini, V. Balzani, A. Credi, M. T. Gandolfi, M. Venturi, *Acc. Chem. Res.* **2001**, *34*, 445.

[12] a) A. P. de Silva, H. Q. N. Gunaratne, C. P. McCoy, *Chem. Commun.* **1996**, 2399; b) L. Fabbrizzi, M. Licchelli, C. Rospo, D. Sacchi, M. Zema, *Inorg. Chim. Acta* **2000**, *300–302*, 453.

[13] a) V. Balzani, A. Credi, G. Mattersteig, O. A. Matthews, F. M. Raymo, J. F. Stoddart, M. Venturi, A. J. P. White, D. J. Williams, *J. Org. Chem.* **2000**, *65*, 1924; b) P. R. Ashton, V. Balzani, A. Credi, G. Mattersteig. S. Menzer, M. B. Nielsen, F. M. Reymo, J. F. Stoddart, M. Venturi,

  0947-6539/03/0903-0809 $ 20.00+.50/0

A. J. P. White, D. J. Williams, *J. Am. Chem. Soc.* **1999**, *121*, 3951; c) B. J. Coe, S. Houbrechts, I. Asselberghs, A. Persoons, *Angew. Chem.* **1999**, *111*, 377; *Angew. Chem. Int. Ed.* **1999**, *38*, 366.

[14] a) A. Fernadez-Acerbes, J.-M. Lehn, *Chem. Eur. J.* **1999**, *5*, 3285; b) V. Balzani, A. Credi, F. M. Raymo, J. F. Stoddart, *Angew. Chem.* **2000**, *112*, 3484; *Angew. Chem. Int. Ed.* **2000**, *39*, 3348.

[15] a) V. Amendola, L. Fabbrizzi, C. Mangano, H. Miller, P. Pallavicini, A. Perotti, A. Taglietti, *Angew. Chem.* **2002**, *114*, 2665; *Angew. Chem. Int. Ed.* **2002**, *41*, 2553; b) A. Bencini, M. A. Bernardo, A. Bianchi, M. Ciampolini, V. Fusi, N. Nardi, A. J. Parola, F. Pina, B. Valtancoli, *J. Chem. Soc. Perkin Trans. 2* **1998**, 413; c) S. Shinkai, T. Nakaji, Y. Nishida, T. Ogawa, *J. Chem. Soc.* **1980**, *102*, 5860.

[16] a) E. Bardazzi, M. Ciampolini, V. Fusi, M. Micheloni, N. Nardi, R. Pontellini, P. Romani, *J. Org. Chem.* **1999**, *64*, 1335; b) P. Dapporto, M. Formica, V. Fusi, M. Micheloni, P. Paoli, R. Pontellini, P. Romani, P. Rossi, *Inorg. Chem.* **2000**, *39*, 4663; c) P. Dapporto, M. Formica, V. Fusi, L. Giorgi, M. Micheloni, P. Paoli, R. Pontellini, P. Rossi, *Inorg. Chem.* **2001**, *40*, 6186.

[17] a) J. A. Aguilar, A. B. Descalzo, P. Diaz, V. Fusi, E. Garcia-España, S. V. Luis, M. Micheloni, J. A. Ramirez, P. Romani, C. Soriano, *J. Chem. Soc. Perkin Trans. 2* **2000**, 1187; b) N. Ceccanti, M. Formica, V. Fusi, M. Micheloni, R. Pardini, R. Pontellini, M. R. Tinè, *Inorg. Chim. Acta* **2001**, *321*, 153.

[18] a) P. Dapporto, M. Formica, V. Fusi, M. Micheloni, P. Paoli, R. Pontellini, P. Romani, P. Rossi, B. Valtancoli, *Eur. J. Inorg. Chem.* **2000**, 51; b) P. Dapporto, M. Formica, V. Fusi, L. Giorgi, M. Micheloni, P. Paoli, R. Pontellini, P. Rossi, *Eur. J. Inorg. Chem.* **2001**, 1763.

[19] M. Formica, V. Fusi, L. Giorgi, M. Micheloni, P. Palma, R. Pontellini, *Eur. J. Org. Chem.* **2002**, 402.

[20] a) J. L. Pierre, P. Baret, G. Gellon, *Angew. Chem.* **1991**, *103*, 75; *Angew. Chem. Int. Ed.* **1991**, *30*, 85; b) W. Moneta, P. Baret, J. L. Pierre, *J. Chem. Soc. Chem. Commun.* **1985**, *13*, 899; c) W. Moneta, P. Baret, J. L. Pierre, *Bull. Soc. Chim. Fr.* **1988**, *6*, 995.

[21] F. H. Allen, O. Kennard, Cambridge Structural Database, *Chem. Soc. Perkin Trans. 2* **1989**, 1131.

[22] F. Bockstahl, E. Graf, M. W. Hosseini, D. Suhr, A. De Cian, J. Fischer, *Tetrahedron Letters* **1997**, *43*, 7539.

[23] *Stereochemical and Stereophysical Behaviour of Macrocycles* (Ed.; I. Bernal), Elsevier, Amsterdam, **1987**, pp 34–35.

[24] M. Micheloni, M. Formica, V. Fusi, P. Romani, R. Pontellini, P. Dapporto, P. Paoli, P. Rossi, B. Valtancoli, *Eur. J. Inorg. Chem.* **2000**, 51.

[25] H.-O. Kalinowski, S. Berger, S. Braun, *^{13}C-NMR Spektroskopie*, GTV, Stuggart, **1984**.

[26] a) J. C. Batchelor, J. H. Prestegard, R. J. Cushley, S. R. Lipsy, *J. Am. Chem. Soc.* **1973**, *95*, 6558; b) A. R. Quirt, J. R. Lyerla, I. R. Peat, J. S. Cohen, W. R. Reynold, M. F. Freedman, *J. Am. Chem. Soc.* **1974**, *96*, 570; c) J. C. Batchelor, *J. Am. Chem. Soc.* **1975**, *97*, 3410.

[27] a) V. Balzani, M. Gomez-Lopez, J. F. Stoddart, J. Fraser, *Acc. Chem. Res.* **1998**, *31*, 405; b) F. Pina, A. Roque, M. J. Melo, M. Maestri, L. Belladelli, V. Balzani, *Chem. Eur. J.* **1998**, *4*, 1184.

[28] H. Gilman, J. Swiss, L. C. Cheney, *J. Am. Chem. Soc.* **1940**, *62*, 1963.

[29] M. Ciampolini, P. Dapporto, M. Micheloni, N. Nardi, P. Paoletti, F. Zanobini, *J. Chem. Soc. Dalton Trans.* **1984**, 1357.

[30] N. Walker, D. D. Stuart, *Acta Crystallogr. Sect. A* **1983**, *39*, 158.

[31] A. Altomare, G. Cascarano, C. Giacovazzo, A. Guagliardi, M. C. Burla, G. Polidori, M. Camalli, *J. Appl. Crystallogr.* **1994**, *27*, 435.

[32] G. M. Sheldrick, SHELXL-97, **1997**, University of Gottingen, Germany.

[33] *International Tables for X-ray Crystallography, Vol.4*, **1974**, Kynoch Press, Birmingham, UK.

[34] M. Nardelli, *Comput. Chem.*, **1983**, *7*, 95.

[35] L. J. Farrugia, *J. Appl. Crystallogr*. **1997**, *30*, 565.

[36] Biosym/MSI, 9685 Scranton Road, San Diego, CA 92121-3752, USA.

[37] C. Janiak, *J. Chem. Soc. Dalton Trans.* **2000**, 3885

[38] C. Bazzicalupi, A. Bencini, A. Bianchi, V. Fusi, C. Giorgi, V. Valtancoli, F. Pina, M. A. Bernardo, *Inorg. Chem.* **1999**, *37*, 3830.

[39] M. Fontanelli, M. Micheloni, *I Spanish-Italian Congr. Thermodynamics of Metal Complexes*, Peñiscola, June 3–6, **1990**, Univ. of Valencia Spain, 41.

[40] a) G. Gran, *Analyst* **1952**, *77*, 661; b) F. J. Rossotti, H. Rossotti, *J. Chem. Educ.* **1965**, *42*, 375.

[41] P. Gans, A. Sabatini, A. Vacca, *Talanta* **1996**, *43*, 1739.

Received: May 21, 2002
Revised: October 24, 2002 [F4110]

  0947-6539/03/0903-0810 $ 20.00+.50/0